Tyrosine phosphorylation acts as a molecular switch to full-scale activation of the eIF2α RNA-dependent protein kinase

Qiaozhu Su, Shuo Wang, Dionissios Baltzis, Li-Ke Qu, Andrew Hoi-Tao Wong*, and Antonis E. Koromilas†

Lady Davis Institute for Medical Research, McGill University, Sir Mortimer B. Davis Jewish General Hospital, Montreal, QC, Canada H3T 1E2

Edited by George R. Stark, Cleveland Clinic Foundation, Cleveland, OH, and approved November 8, 2005 (received for review September 20, 2005)

Phosphorylation of the α-subunit of translation eukaryotic initiation factor-2 (eIF2) leads to the inhibition of protein synthesis in response to diverse conditions of stress. Serine/threonine RNA-dependent protein kinase (PKR) is an eIF2α kinase family member induced by type I IFN and activated in response to dsRNA or virus infection. Herein, we demonstrate that human PKR is a dual specificity kinase phosphorylated at Y101, Y162 and Y293 *in vitro* and *in vivo*. Site-specific tyrosine phosphorylation is essential for efficient dsRNA-binding, dimerization, kinase activation and eIF2α phosphorylation of PKR. Biologically, tyrosine phosphorylation of PKR mediates the antiviral and antiproliferative properties of the kinase through its ability to control translation. Our data demonstrate an important role of tyrosine phosphorylation in biochemical and biological processes caused or mediated by the activation of the eIF2α kinase PKR.

cell proliferation | protein phosphorylation | translational control | virus infection

Regulation of gene expression at the translational level plays critical roles in cell proliferation and apoptosis (1). Most of translational control is known to be exerted at the level of initiation (2). An important mechanism of initiation proceeds through the regulation of eukaryotic initiation factor-2 (eIF2) activity, whose phosphorylation on S51 of its α-subunit results in the inhibition of protein synthesis (2). Mammalian cells contain a family of eIF2α kinases and, among them, RNA-dependent protein kinase (PKR) is the most widely studied member (2). PKR is a 68-kDa polypeptide in humans and a 65-kDa polypeptide in mice, and it binds dsRNA with high affinity (3). The structural features of PKR include an N terminus dsRNA-binding domain and a C terminus kinase domain (KD) (3). The dsRNA-binding domain contains two dsRNA-binding motifs (dsRBMs) that are located at amino acids 10–78 and 101–168 in human PKR (3). The current model of PKR activation proposes latent PKR is in a folded "locked" conformation through an intermolecular interaction between the dsRBM II and KD (4, 5). Binding of dsRNA to dsRBM I induces conformational changes that promote the cooperative binding of dsRBM II to dsRNA and expose the KD (4, 5). These conformational alterations facilitate PKR dimerization through hydrophobic side-chain interactions between the regions at amino acids 244–296 of two kinase molecules, leading to autophosphorylation at multiple serine and threonine sites (3–5). PKR expression is transcriptionally induced by type I IFN (i.e., IFN-α/β) (6), a property associated with the antiviral and antiproliferative actions of the kinase (7). Consistent with its antiviral property, ectopic expression of PKR in various mouse and human cell lines confers resistance to infection by a variety of viruses by eliciting a strong IFN response (7). Activation of PKR leads to the inhibition of cell proliferation and destruction of cells by apoptosis (8), whereas inhibition of PKR activity by dominant negative mutants facilitates malignant transformation and the induction of tumorigenesis (9).

Although PKR has been characterized as a serine/threonine kinase, two reports provided biochemical evidence for its possible regulation by tyrosine phosphorylation. First, Icely *et al.* (10) were able to clone mouse PKR using anti-phosphotyrosine Abs. Second, Lu *et al.* (11) demonstrated the tyrosine autophosphorylation of PKR in bacteria and budding yeast. Although these observations implied a dual specificity for PKR, they did not address the role of tyrosine phosphorylation in regulation of the kinase activity nor did they investigate the biological relevance of PKR tyrosine phosphorylation in cell proliferation, virus replication, and regulation of protein synthesis. Herein, we demonstrate that human PKR is a dual specificity kinase whose phosphorylation at Y101, Y162 and Y293 have profound effects on its biochemical and biological functions.

Results

First, we verified the tyrosine phosphorylation of PKR *in vitro*. Active GST–PKR was treated with calf intestinal phosphatase (CIP) to remove preexisting autophosphorylated sites and then subjected to kinase reaction in the presence of [^{32}P-γ]ATP. Phosphoamino acid analysis of the ^{32}P-labeled kinase indicated the presence of phosphoserine, phosphothreonine, and phosphotyrosine residues (Fig. 1*A*). To verify tyrosine phosphorylation, active GST–PKR was treated with a recombinant GST fusion protein consisting of human T cell tyrosine phosphatase (TC-PTP) (Fig. 1B) (12). We found that treatment with the tyrosine phosphatase eliminated the tyrosine phosphorylation of GST–PKR WT (Fig. 1*B*, lane 1 of row a) as opposed to treatment with the catalytic mutant of the tyrosine phosphatase GST–TC-PTPD182A, which did not affect tyrosine autophosphorylation of the kinase (Fig. 1*B*, lane 3 of row a). Also, detection of the kinase-defective GST–PKRK296R by anti-phosphotyrosine Abs was not possible (Fig. 1*B*, lanes 2 and 4 of row a), further suggesting that PKR protein does not contain an epitope that mimics tyrosine phosphorylation. Tyrosine-phosphorylated PKR was also detected in mammalian cells. That is, 2D gel electrophoresis and immunoblotting with an anti-phosphotyrosine Ab detected the tyrosine phosphorylation of PKR in human HT1080 cells (Fig. 1*C*, spots c–e of row a). In addition, the fractions of PKR recognized by the anti-phosphotyrosine Ab were shifted to more acidic areas of the gel, suggesting that the hyperphosphorylated forms of the kinase contained tyrosine-phosphorylated protein. We also obtained evidence that tyrosine

BIOCHEMISTRY

Conflict of interest statement: No conflicts declared.

This paper was submitted directly (Track II) to the PNAS office.

Abbreviations: CIP, calf intestinal phosphatase; dsRBM, dsRNA-binding motifs; eIF2, eukaryotic initiation factor-2; KD, kinase domain; MEF, mouse embryonic fibroblast; PKR, RNA-dependent protein kinase; TC-PTP, human T cell phosphatase; VSV, vesicular stomatitis virus.

*Present address: Memorial Sloan-Kettering Cancer Center, New York, NY 10021.

†To whom correspondence should be addressed at: Lady Davis Institute for Medical Research, Jewish General Hospital, 3755 Côte-Ste-Catherine Street, Montreal, QC, Canada H3T 1E2. E-mail: antonis.koromilas@mcgill.ca.

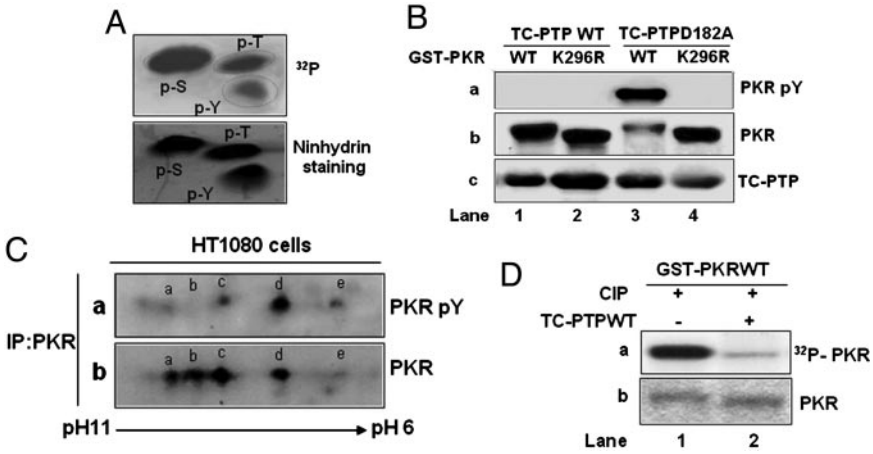

Fig. 1. Tyrosine phosphorylation of PKR *in vitro* and *in vivo*. (*A*) Two-dimensional phosphoamino acid analysis of GST–PKR. GST–PKRWT (10 ng) was treated with CIP followed by autophosphorylation in the presence of [γ-^{32}P] ATP. The phosphorylated protein was subjected to phosphoamino acid analysis as described in *Supporting Materials and Methods*. The positions of radioactive (*Upper*) and total phosphoamino acids (*Lower*) are as follows: pS, phosphoserine; pT, phosphothreonine; and pY, phosphotyrosine. (*B*) Ten ng of GST–PKR WT (lanes 1 and 3) or GST–PKRK296R (lanes 2 and 4) was incubated with 10 ng of GST–TC-PTP WT (lanes 1 and 2) or the catalytically inactive GST–TC-PTP D182A (lanes 3 and 4). Proteins were immunoblotted with anti-phosphotyrosine 4G10 mAb (row a), anti-human PKR mAb (row b) or anti-TC-PTP mAb (row c). (*C*) Protein extracts (1 mg) from HT1080 cells were immunoprecipitated with anti-human PKR mAb followed by 2D gel electrophoresis and immunoblotting with either anti-phosphotyrosine 4G10 mAb (row a) or anti-human PKR mAb (row b). (*D*) Tyrosine phosphorylation is required for PKR kinase activity. GST–PKRWT (10 ng) was treated with CIP followed by incubation with either GST alone (lane 1) or GST–TC-PTP WT (lane 2). GST–PKR WT was then subjected to autophosphorylation in the presence of [γ-^{32}P]ATP. Radioactive bands were visualized by autoradiography (row a) whereas GST–PKR WT levels by Coomassie blue staining of the gel (row b).

phosphorylation played a role in kinase activation. For example, treatment of GST–PKR WT with CIP, which targets phosphorylated serine, threonine, and tyrosine residues, resulted in a kinase that retained its capacity to be activated by autophosphorylation (Fig. 1*D*, lane 1 of row a). However, the autophosphorylation capacity of the CIP-treated GST–PKR WT was significantly reduced by the presence of GST–TC-PTP (Fig. 1*D*, lane 2 of row a), thus indicating that tyrosine phosphorylation is required for optimal activation of the kinase.

When the sequences of mouse, human, and rat PKR proteins were compared, we noticed that several tyrosine residues were highly conserved between these species (data not shown). Among the conserved residues, Y293 attracted our attention because it lies within the catalytic subdomain II, which is involved in ATP binding (13) (Fig. 6*A*, which is published as supporting information on the PNAS web site). In addition, Y293 is located three residues upstream of the invariant K296, which is essential for the enzymatic activity of PKR (14). We also focused on the N terminus of PKR and, specifically, on the conversed Y101 and Y162 within the dsRBM II of the human kinase (Fig. 6*A*). This motif contains an α-β-β-β-α fold with the two α-helices lying on each side and being packed against a three-stranded antiparallel β-sheet (Fig. 6*B*) (4). A negative charge generated by phosphorylation at these tyrosines could cause an expulsion of the two α-helices and result in structural alterations that could possibly affect dsRNA binding and/or kinase activity. To test whether the above tyrosine residues are phosphorylated, we generated Abs against phosphotyrosine-containing peptides encompassing Y101 (pY101 phosphopeptide), Y162 (pY162 phosphopeptide), or Y293 (pY293 phosphopeptide) of human PKR. First, we examined the suitability of these Abs for detecting active PKR by immunoblotting (Fig. 2). We noticed that the anti-PKRpY101 Ab recognized GST–PKR WT (Fig. 2*A*, lane 1 of row a) but not the catalytically inactive GST–PKRK296R (Fig. 2*A*, lane 2 of row a). However, recognition of GST–PKR WT by anti-PKRpY101 Ab was lost when the pY101 phosphopeptide was present (Fig. 2*A*, lane 3 of row a). Contrary to pY101 phosphopeptide, the presence of the nonphosphorylated Y101 peptide was not able to block the detection of active GST–PKR with the anti-PKRpY101 Ab (Fig. 2*A*, lane 5). Similarly, active GST–PKR was recognized by the anti-PKRpY162 Ab (Fig. 2*B*, lane 1 of row a) or anti-PKRpY293 Ab (Fig. 2*C*, lane 1 of row a), and this recognition was abolished by the presence of the pY162 phosphopeptide (Fig. 2*B*, lane 3 of row a) or the pY293 phosphopeptide (Fig. 2*C*, lane 3 of row a), respectively. However, each of these two anti-phosphotyrosine Abs was not blocked by the presence of the corresponding nonphosphorylated peptide (Fig. 2 *B* and *C*, lane 5). Furthermore, recognition by each of the three phosphospecific Abs was not blocked by the presence of phosphopeptides used to generate the other two Abs (Fig. 7 *A–C*, which is published as supporting information on the PNAS web site), thus further demonstrating their specificity. Phosphorylation at Y101, Y162, and Y293 was further verified by incubating GST–PKR WT with GST–TC-PTP WT or GST–TC-PTP D182A (Fig. 2 *D–F*). Treatment with GST–TC-PTP WT resulted in the loss of the phosphospecific signal of the active kinase with the anti-PKRpY101 Ab (Fig. 2*D*, lane 1 of row a), anti-PKRpY162 Ab (Fig. 2*E*, lane 1 of row a), or anti-PKRpY293 Ab (Fig. 2*F*, lane 1 of row a). Contrary to WT phosphatase, incubation with the catalytically inactive GST–TC-PTP D182A did not affect GST–PKR WT autophosphorylation at Y101, Y162, or Y293 (Fig. 2 *D–F*, lane 3 of row a). Furthermore, immunodepletion of GST–PKR showed that $\approx$10% of the kinase is phosphorylated at each tyrosine residue *in vitro* (Fig. 7*D*). We also found that human PKR was phosphorylated at all three tyrosine sites in HT1080 cells and that this site-specific phosphorylation was further induced after prolonged treatment with IFN-α in an attempt to enhance detection by up-regulating endogenous PKR (Fig. 3). These data demonstrated that Y101, Y162, and Y293 of PKR are phosphorylated both *in vitro* and *in vivo*.

We next investigated the functionality of tyrosine-phosphorylated PKR by examining the activity of PKR mutants bearing tyrosine-to-phenylalanine substitutions. Using GST fusion proteins, we found that the Y101F mutation partially diminished ($\approx$20%) the autophosphorylation levels of the kinase (Fig. 4*A*, lane 3 of row a), although eIF2α phosphorylation by GST–PKRY101F was as efficient as phosphorylation by GST–PKR

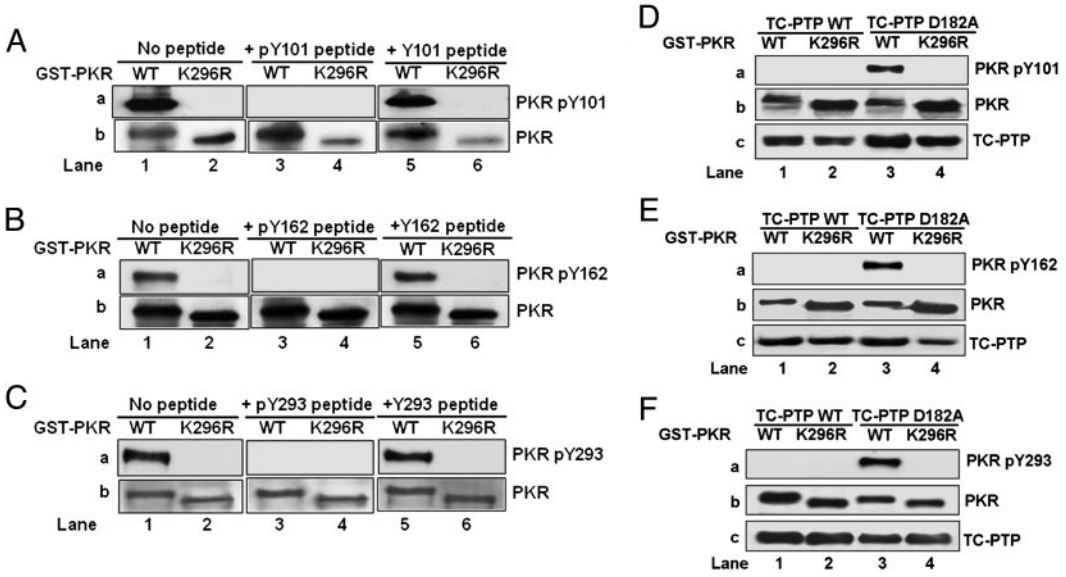

Fig. 2. PKR autophosphorylates on Y101, Y162, and Y293 *in vitro*. (*A–C*) GST–PKR WT (lanes 1, 3, and 5) or GST–PKRK296R (lanes 2, 4, and 6) was immunoblotted with an affinity-purified rabbit polyclonal Ab against phosphoY101 (PKR pY101; *A*, row a), phosphoY162 (PKR pY162; *B*, row a) or phosphoY293 (PKR pY293; *C*, row a) either in the absence (*A–C*, row a, lanes 1 and 2) or presence of the corresponding phosphorylated (row a, lanes 3 and 4) or nonphosphorylated peptides (row a, lanes 5 and 6). GST–PKR levels were detected by immunoblotting with anti-human PKR mAb (*A–C*, row b). (*D–F*) Dephosphorylation of GST–PKR by GST–TC-PTP *in vitro*. The experiment was performed as in Fig. 1*A* with the exception that immunoblotting was performed with anti-PKR pY101 Ab (*D*, row a), anti-PKR pY162 Ab (*E*, row a) or anti-PKR pY293 Ab (*F*, row a).

WT (Fig. 4*A*, compare lanes 1 and 3 of row b). In contrast, the Y162F or Y101F/Y162F mutation(s) exhibited a higher inhibitory effect on PKR autophosphorylation (≈60%) (Fig. 4*A*, lanes 4 and 5 of row a), which correlated with a significant reduction (≈80%) in eIF2α phosphorylation by each GST–PKR mutant compared with GST–PKR WT (Fig. 4*A*, compare lane 1 with lanes 4 and 5 of row b). Interestingly, the Y293F mutation conveyed a strong inhibitory effect on PKR autophosphorylation (Fig. 4*A*, lane 3 of row d) and substrate phosphorylation (Fig. 4*A*, lane 3 of row e), indicating that Y293 is critical for kinase activity. Furthermore, the overall tyrosine phosphorylation of the GST–PKR tyrosine mutants was reduced. That is, we found

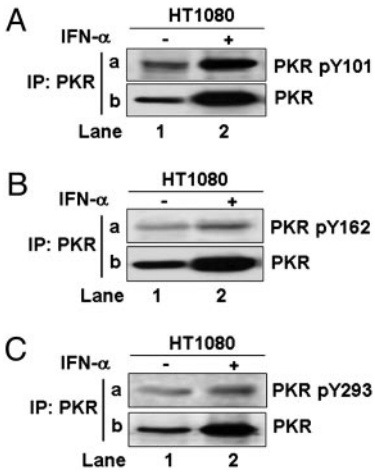

Fig. 3. PKR phosphorylation at Y101, Y162, and Y293 *in vivo*. Human fibrosarcoma HT1080 cells were left untreated (lane 1) or treated with human IFN-α (1,000 units/ml) for 16 h (lane 2). Protein extracts (250 μg) were subjected to immunoprecipitation (IP) with anti-human PKR (F9) mAb followed by immunoblotting with either anti-PKR pY101 Ab (*A*, row a), anti-PKR pY162 Ab (*B*, row a), or anti-PKR pY293 Ab (*C*, row a). PKR protein levels were detected by immunoblotting with anti-human PKR (F9) mAb (row b).

that the Y101F and/or Y162F mutation(s) diminished the tyrosine phosphorylation levels of GST–PKR by ≈50% compared with WT kinase (lanes 3–5 of row a in Fig. 8*A*, which is published as supporting information on the PNAS web site), whereas tyrosine phosphorylation of either GST–PKRY293F (Fig. 8*A*, lane 6 of row a) or the catalytic inactive GST–PKRK296R (Fig. 8*A*, lane 2 of row a) was barely detectable. Site-specific tyrosine phosphorylation of PKR also plays a role in kinase dimerization because GST–PKR tyrosine mutants were partially defective (≈40%) in their interaction with PKR WT (Fig. *4B*). In line with the dimerization effects, dephosphorylation of GST–PKR WT with TC-PTP prevented its interaction with Flag-PKR WT (Fig. 8*B*), further supporting a positive role of tyrosine phosphorylation in kinase dimerization. When the catalytic activities of Flag–PKR tyrosine mutants were tested in PKR$^{-/-}$ mouse embryonic fibroblasts (MEFs) (15), we found that autophosphorylation of Flag–PKRY101F or Flag-PKRY162F was diminished by ≈50% (Fig. 4*C*, lanes 4 and 5 of row a), whereas Flag-PKRY293F autophosphorylation was reduced to almost undetectable levels (Fig. 4*C*, lane 6 of row a). We also noticed that the dsRNA-binding capacity of Flag–PKR tyrosine mutants was partially (≈50%) defective compared with Flag–PKR WT (Fig. 4*D*) as was the dsRNA-binding activity of the catalytic inactive Flag-PKRK296R (Fig. 4*D*, compare lanes 3–6 with lane 2). Collectively, these data suggested that site-specific tyrosine phosphorylation is required for efficient dsRNA-binding, dimerization, and activation of PKR.

Next, we addressed the function of PKR tyrosine mutants in cell proliferation by performing colony formation assays in PKR$^{-/-}$ MEFs (Fig. 5*A*, row a) (15). The colony formation efficiency with the vector DNA (control) was arbitrarily set to 100%. We observed that colony formation with the catalytic inactive Flag-PKRK296R or Flag-PKRY293F was almost 100%. However, cells expressing the Flag-PKRY101F or Flag-PKRY162F were less efficient in forming colonies (70–90%) than were control cells. Contrary to Flag-PKR mutants, colony formation with Flag-PKR WT was poor because of the strong antiproliferative effects of the WT kinase. Similar results were

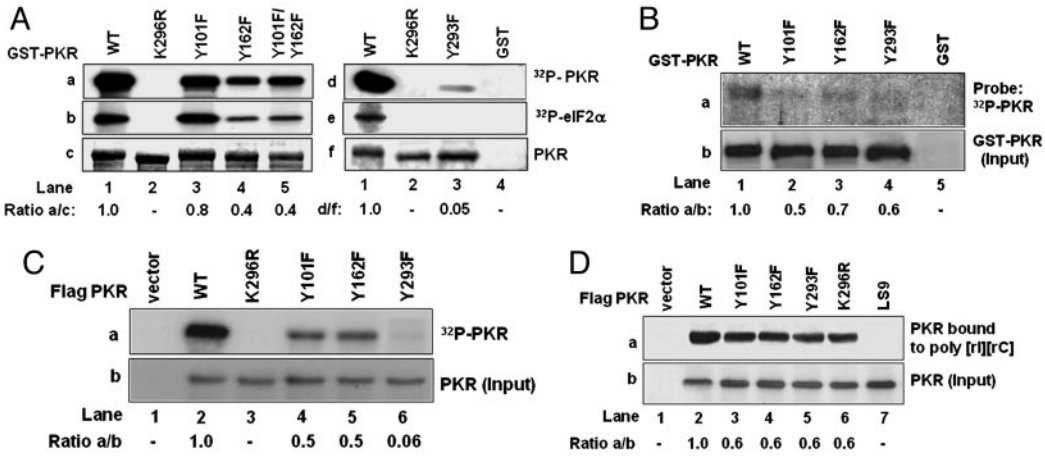

Fig. 4. Biochemical properties of PKR tyrosine mutants. (*A*) Catalytic activity of human PKR tyrosine variants *in vitro*. Purified GST–PKR proteins (10 ng) bearing the indicated mutations were subjected to autophosphorylation in the presence of 10 ng of purified histidine-tagged eIF2α and [γ-^{32}P]ATP. Half of the reactions were subjected to SDS/PAGE and autoradiography to detect phosphorylated GST–PKRs (rows a and d) or eIF2α (rows b and e), and the rest was used for immunoblotting with anti-human PKR (F9) mAb and enhanced chemiluminescence (1-min exposure) (rows c and f). The ratio of autophosphorylated GST–PKRs (rows a and c) to total protein (rows d and f) is indicated. (*B*) Interaction of PKR tyrosine mutants with WT kinase. Purified GST or GST–PKR proteins (10 ng) bearing the indicated mutations were subjected to far-Western analysis using recombinant ^{32}P-PKR WT as a probe. Radioactive bands were visualized by autoradiography (row a), and protein levels were visualized by immunoblotting (row b). The ratio of GST–PKR bound to ^{32}P-PKR versus the total protein is indicated. (*C*) Analysis of PKR tyrosine mutants in PKR$^{-/-}$ MEFs. Cells were transiently transfected with 2 μg of pcDNA3.1/zeo plasmid containing the indicated Flag–PKR forms. Protein extracts were subjected to immunoprecipitation with anti-Flag Ab followed by autophosphorylation in the presence of [γ-^{32}P]ATP. Radioactive bands were visualized by autoradiography (row a), and Flag-PKR levels were detected by immunoblotting with anti-Flag mAb (row b). The ratio of autophosphorylated versus total Flag-PKR protein is indicated. (*D*) dsRNA-binding activity of PKR tyrosine mutants. The proteins were expressed as in *C* and were subjected to pull-down assays with poly[rI][rC]-agarose followed by immunoblotting with anti-Flag mAb (row a). Flag-PKR levels in 50 μg of the protein extracts used for the pull-down (input) were detected by immunoblotting with anti-Flag Ab (row b).

obtained in human HT1080 cells (data not shown), showing that control of cell proliferation by the PKR tyrosine mutants is not cell-type- or species-specific. Therefore, efficient tyrosine phosphorylation is necessary for the antiproliferative action of PKR.

We also examined the translational properties of the PKR tyrosine mutants. Translation was assessed by measuring β-galactosidase reporter gene activity in HT1080 cells cotransfected with each of the Flag-PKR mutants (Fig. 5*B*) (16). We observed that PKR proteins bearing a Y101F, Y162F, or Y101F/Y162F mutation(s) had partial inhibitory effects on protein synthesis compared with Flag-PKR WT (Fig. 5*B*). In contrast, Flag-PKR Y293F exhibited the same ability to control the translation of the reporter gene as the catalytic inactive Flag-PKRK296R (Fig. 5*B*). These data implied that tyrosine phosphorylation of PKR positively contributes to the inhibition of protein synthesis by the active kinase. Given the antiviral properties of PKR, we further investigated the function of PKR tyrosine mutants in cells infected with vesicular stomatitis virus (VSV). Specifically, we tested the ability of the PKR tyrosine mutants to modulate eIF2α phosphorylation in PKR$^{-/-}$ MEFs infected with VSV (Fig. 5*C*). We noticed that eIF2α phosphorylation was more highly induced in VSV-infected cells expressing Flag-PKR WT (Fig. 5*C*, lane 8 of row b) than in control cells (Fig. 5*C*, lane 7 of row b) or cells expressing the PKR tyrosine mutants (Fig. 5*C*, lanes 9–11 of row b). Similar to tyrosine mutants, induction of eIF2α phosphorylation was not possible in cells expressing the catalytic inactive Flag-PKRΔ6 (17), which served as a negative control. To verify the antiviral function of PKR tyrosine phosphorylation, we performed plaque formation assays (18) to measure VSV production in HEK293 cells transiently expressing each of the Flag-PKR mutants (Fig. 5*D*). We found that expression of Flag-PKR WT suppressed VSV replication by a factor of 10^4 to 10 plaque-forming units/ml compared with cells transfected with vector DNA alone (Fig. 5*D*). Contrary to Flag-PKR WT, each of the Flag-PKR tyrosine mutants, as well as the catalytically inactive Flag-PKRK296R, failed to suppress VSV replication. Virus replication was partially restored only in cells expressing Flag-PKR Y101F at 24 h after infection. These findings revealed a role of PKR tyrosine phosphorylation in the inhibition of VSV replication.

Discussion

Herein, we demonstrate the dual specificity of PKR and identify three tyrosine residues whose phosphorylation controls the biochemical and biological properties of the kinase. Using phosphospecific Abs, we show the phosphorylation of PKR at Y101, Y162, and Y293 *in vitro* and *in vivo*. Immunodepletion experiments indicated that $\approx$10% of PKR is phosphorylated at each tyrosine residue *in vitro* (Fig. 7*D*), although the stoichiometry of phosphorylation at each specific residue *in vivo* has not been determined. Y101 and Y162 flank the dsRBM II, which spans amino acids 101 and 167 in the human polypeptide (3). Based on structural data of the N terminus dsRNA-binding region of PKR, we hypothesized that phosphorylation at Y101 and Y162 might be involved in dsRNA binding and consequently kinase activation. Consistent with this notion, functional characterization of Y101F and Y162F mutants revealed that phosphorylation at these sites is needed for efficient dsRNA binding and kinase dimerization and activation. Y293 is located within the kinase subdomain II of PKR and is conserved among the orthologs (Fig. 6*A*) and homologs of PKR (Fig. 9*A*, which is published as supporting information on the PNAS web site). The introduction of the Y293F mutation causes significant defects in PKR autophosphorylation and eIF2α phosphorylation, providing evidence for a critical function of this phosphorylated residue.

Analysis of the biological function showed that tyrosine phosphorylation is required for the antiproliferative and antiviral activities of PKR. Although both activities of the kinase have been shown to proceed through eIF2α phosphorylation, our findings provide evidence that tyrosine phosphorylation can modulate PKR function independently of eIF2α phosphoryla-

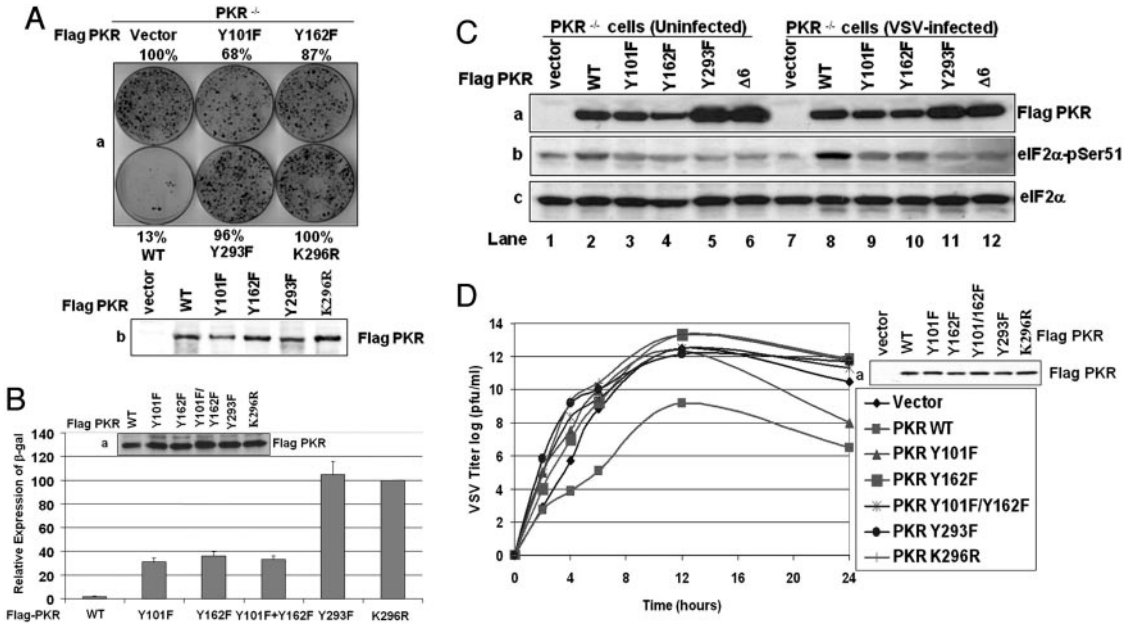

Fig. 5. Biological relevance of PKR tyrosine phosphorylation. (*A*) Colony formation assays. PKR$^{-/-}$ MEF cells were transfected with 2 μg of pcDNA3.1/zeo plasmid containing the indicated forms of Flag-PKR. Transfected cells were maintained in 300 μg/ml zeocin for 2 weeks, and viable colonies were fixed and stained with crystal violet (row a). The protein levels of Flag-PKR proteins expressed 2 days after transfection were detected by immunoprecipitation and immunoblotting with anti-Flag Ab (row b). (*B*) Translational control by the PKR tyrosine mutants. HT1080 cells were transiently transfected with 1 μg of pEF-β-galactosidase DNA together with 1 μg of pcDNA3/zeo plasmid DNA either lacking or containing the indicated forms of Flag-PKR. Thirty-two hours after transfection, β-galactosidase activity was measured in protein extracts expressing each of the PKR mutants and normalized to β-galactosidase activity in cells expressing Flag-PKRK296R, whose translation efficiency was set to 100%. The data represent the average of two independent experiments performed in duplicate. Expression of Flag-PKR proteins was detected by immunoblotting (row a). (*C* and *D*) The antiviral properties of PKR tyrosine mutants. (*C*) PKR$^{-/-}$ MEF cells were transfected with 2 μg of pcDNA3.1/zeo plasmid containing the indicated forms of Flag-PKR cDNA. Thirty-six hours after transfection, cells were left uninfected or infected with VSV at MOI 10. Cells were harvested 24 h later, and equal protein extracts were subjected to immunoblotting with anti-Flag mAb (row a), antiphosphoS51 eIF2α polyclonal Ab (row b), or anti-eIF2α polyclonal Ab (row c). (*D*) HEK293 cells were transiently transfected with 2 μg of pcDNA3.1/zeo plasmid containing the indicated forms of Flag-PKR cDNA. Plaque formation assays after VSV infection were performed as described in ref. 18 (see also *Supporting Materials and Methods*). The protein levels of Flag-PKR proteins were detected by immunoblotting.

tion. Specifically, the Y101F mutation impairs the translational, antiproliferative and antiviral activities of PKR without affecting the ability of the PKR mutant to phosphorylate eIF2α. One possibility is that tyrosine phosphorylation functions as a switch for substrate specificity of PKR. Another possibility is that tyrosine phosphorylation is needed for the signaling properties of PKR through interactions with Src homology 2-containing proteins that could serve as substrates of the kinase. Consistent with this notion, it is of interest that the Src homology 2 containing protein Nck-1 controls mRNA translation through its functional and physical interactions with eIF2 (19, 20).

Structural analysis of several kinases has shown that their folding properties are evolutionarily conserved (21, 22). The proteins fold in two separate domains or lobes; the small N-terminal lobe is composed of a five-stranded β-sheet and one prominent α-helix, named helix αC, whereas the C-terminal lobe is larger and predominantly helical (21). Recent studies on the 3D structure of KD of PKR showed that conformation of the $P+1$ loop in the kinase activation region adopts an extreme outward orientation from residues 448–452, approximating that of a tyrosine kinase (23). Preceding and following this region, the activation segment of PKR returns to a canonical serine/threonine protein kinase conformation (23). The unique distortion of $P+1$ loop may relate to the ability of PKR to phosphorylate on serine/threonine residues and tyrosine residues, consistent with its function as a dual-specificity kinase. Most dual-specificity protein kinases employ a $P+1$ loop signature motif diagnostic of serine/threonine-directed protein kinase activity and display the ability to phosphorylate serine/threonine residues and tyrosine residues (23). This unique and more flexible structure endows PKR with a unique activation site that can accommodate tyrosine substrates and serine/threonine substrates (23). Y293 lies within the VAIK motif, which contains K296, which coordinates ATP binding and is buried in the dimer interface of the two KDs (23). Based on the structural data of KD only, the hydroxyl group of Y293 does not appear to be readily accessible for phosphorylation (23). Moreover, the introduction of a bulky phosphate at Y293 is expected to impede KD dimerization. However, because the dsRNA-binding domain and the long $\beta4$–$\beta5$ linger of PKR were omitted from the structural analysis, the remainder KD molecule may be disordered (24). As such, the reported structural data may not fully represent the conformation of the KD in the full-length kinase (24). Binding of dsRNA to PKR induces conformational changes (4, 5), which may expose Y293 and make it more accessible for phosphorylation. A large number of known serine/threonine and tyrosine kinases contain a tyrosine residue located three residues upstream of the invariant lysine within the catalytic subdomain II (25) (Fig. 9*A*). Introduction of the Y69F mutation in the catalytic subunit of the serine/threonine protein kinase A did not affect its catalytic activity (Fig. 9*B*), indicating that tyrosine-to-phenylalanine substitution in this position does not exhibit deleterious effects on other kinases and is unlikely to affect ATP binding.

The crystallographic studies of the KD of PKR also have led to a model that favors the trans-interdimer autophosphorylation of PKR in which dimers phosphorylate dimmers (26). From these studies, autophosphorylation of PKR on T446 enhances its catalytic activity and is essential for specific recognition of eIF2α. Our findings show that tyrosine phosphorylation is

needed for optimal T446 phosphorylation (Fig. 8*C*) perhaps through structural alterations that facilitate trans-interdimer formation and/or maintain the kinase in an active conformation. Such conformational changes have been shown to take place in the activation of other kinases, including the EphB2 receptor tyrosine kinase and the type I TGFβ receptor (TβR-I). Specifically, EphB2 receptor tyrosine kinase contains an N-terminal juxtamembrane region, which, in its unphosphorylated form, can act as a negative regulator (27) by stabilizing the N-terminal lobe of the kinase in an inactive conformation (28). In contrast, the TβR-I, a receptor serine/threonine kinase, also contains an N-terminal regulatory segment, called the GS region, which, in its unphosphorylated form, can inhibit kinase activity when bound by the inhibitory protein FKBP12 (29–31). When bound to FKBP12, the GS acquires a conformation that helps to maintain the N-terminal lobe of the kinase in a distorted inactive conformation (31). These structural alterations of EphB2 and TβR-I mediated by the N-terminal domains disrupt productive ATP bindings. For PKR, the three-dimensional structure of the whole kinase molecule has not as yet been resolved, and this adds more to the complexity of the interpretation of the role of tyrosine phosphorylation in the folding and conformational changes of the kinase.

The identification of PKR as a dual-specificity kinase is a finding with important implications in the diverse biological roles proposed for it. As tyrosine phosphorylation is involved in various cellular signal transduction pathways, it is tempting to speculate that the defects in signal transduction pathways and gene expression associated with human disease are due, at least in part, to modifications of PKR tyrosine kinase activity. It will be significant to identify tyrosine-phosphorylated substrates of PKR and provide a better insight for physiological role of the tyrosine kinase activity of PKR.

Materials and Methods

Generation of Anti-Phosphotyrosine 101, 162, and 293 Abs of Human PKR. Rabbit antiserum was produced against three chemically synthesized phosphopeptides GLSMGNpY^{101}IGLINR, LAAKLApY^{162}LQILSE, and RIDGKTpY^{293}VIKRVK (where pY represents phosphotyrosine) of human PKR conjugated with keyhole limpet hemocyanin. Production of Abs in the serum from various bleeds was quantified by ELISA. Serum with the highest titer was pooled and purified by negative preadsorption against the nonphosphorylated form of each peptide. The final products were generated by affinity chromatography using the corresponding phosphorylated peptide at Y101, Y162, and Y293.

Immunoprecipitation and Immunoblot analysis. Immunoprecipitation and immunoblotting were performed as described in ref. 32. The following Abs were used: anti-phosphotyrosine 4G10 mouse mAb (Upstate Biotechnology, Lake Placid, NY), anti-hemagglutinin 12CA5 mouse mAb (Roche), anti-human PKR mouse monoclonal F9 mAb (16), anti-GST rabbit polyclonal Ab (Amersham Pharmacia), anti-TC-PTP mouse mAb (33), anti-eIF2α rabbit polyclonal Ab (Cell Signaling Technology), anti-phosphoS51 of eIF2α rabbit polyclonal Ab (16), anti-FLAG (M2) mouse mAb (Sigma), anti-phosphoT446 of human PKR (anti-PKRpT446) rabbit polyclonal Ab (Upstate Biotechnology), anti-phosphoY101 of human PKR (anti-PKRpY101) polyclonal Ab, anti-phosphoY162 of human PKR (anti-PKRpY162) polyclonal Ab, anti-phosphoY293 of human PKR (anti-PKRpY293) polyclonal Ab, Ab against the catalytic D subunit of PKA (C-20; Santa Cruz Biotechnology). All Abs were used at a final concentration of 0.1–1 μg/ml. After incubation with horseradish peroxidase-conjugated anti-mouse or anti-rabbit IgG Abs (1:1,000 dilution, Amersham Pharmacia Biotech), proteins were visualized with the enhanced chemiluminescence detection system according to the manufacturer's instructions (ECL, Amersham Pharmacia Biotech). Quantification of the bands in the linear range of exposure was performed by densitometry using the National Institutes of Health IMAGE 1.54 software.

Further experimental details are listed in *Supporting Materials and Methods*, which is published as supporting information on the PNAS web site.

We thank S. Richard for guidance with the phosphoamino acid analysis and helpful suggestions and S. Taylor for the catalytic subunit PKA cDNA. This work was supported by a grant from the Cancer Research Society of Canada (to A.E.K.). D.B. is a research student of the Terry Fox Foundation through an award from the National Cancer Institute of Canada and a recipient of the Canadian Institutes of Health Research Cancer Consortium Training Grant Studentship Award.

1. Holcik, M. & Sonenberg, N. (2005) *Nat. Rev. Mol. Cell. Biol.* **6,** 318–327.
2. Dever, T. E. (2002) *Cell* **108,** 545–556.
3. Clemens, M. J. & Elia, A. (1997) *J. Interferon Cytokine Res.* **17,** 503–524.
4. Nanduri, S., Rahman, F., Williams, B. R. & Qin, J. (2000) *EMBO J.* **19,** 5567–5574.
5. Nanduri, S., Carpick, B. W., Yang, Y., Williams, B. R. & Qin, J. (1998) *EMBO J.* **17,** 5458–5465.
6. Stark, G. R., Kerr, I. M., Williams, B. R., Silverman, R. H. & Schreiber, R. D. (1998) *Annu. Rev. Biochem.* **67,** 227–264.
7. Katze, M. G., He, Y. & Gale, M., Jr. (2002) *Nat. Rev. Immunol.* **2,** 675–687.
8. Jagus, R., Joshi, B. & Barber, G. N. (1999) *Int. J. Biochem. Cell Biol.* **31,** 123–138.
9. Lengyel, P. (1993) *Proc. Natl. Acad. Sci. USA* **90,** 5893–5895.
10. Icely, P. L., Gros, P., Bergeron, J. J., Devault, A., Afar, D. E. & Bell, J. C. (1991) *J. Biol. Chem.* **266,** 16073–16077.
11. Lu, J., O'Hara, E. B., Trieselmann, B. A., Romano, P. R. & Dever, T. E. (1999) *J. Biol. Chem.* **274,** 32198–32203.
12. Ibarra-Sanchez, M. J., Simoncic, P. D., Nestel, F. R., Duplay, P., Lapp, W. S. & Tremblay, M. L. (2000) *Semin. Immunol.* **12,** 379–386.
13. Hanks, S. K. & Quinn, A. M. (1991) *Methods Enzymol.* **200,** 38–62.
14. Katze, M. G., Wambach, M., Wong, M. L., Garfinkel, M., Meurs, E., Chong, K., Williams, B. R., Hovanessian, A. G. & Barber, G. N. (1991) *Mol. Cell. Biol.* **11,** 5497–5505.
15. Abraham, N., Stojdl, D. F., Duncan, P. I., Methot, N., Ishii, T., Dube, M., Vanderhyden, B. C., Atkins, H. L., Gray, D. A., McBurney, M. W., *et al.* (1999) *J. Biol. Chem.* **274,** 5953–5962.
16. Li, S. & Koromilas, A. E. (2001) *J. Biol. Chem.* **276,** 13881–13890.
17. Koromilas, A. E., Roy, S., Barber, G. N., Katze, M. G. & Sonenberg, N. (1992) *Science* **257,** 1685–1689.
18. Sharma, S., tenOever, B. R., Grandvaux, N., Zhou, G. P., Lin, R. & Hiscott, J. (2003) *Science* **300,** 1148–1151.
19. Kebache, S., Zuo, D., Chevet, E. & Larose, L. (2002) *Proc. Natl. Acad. Sci. USA* **99,** 5406–5411.
20. Kebache, S., Cardin, E., Nguyen, D. T., Chevet, E. & Larose, L. (2004) *J. Biol. Chem.* **279,** 9662–9671.
21. Huse, M. & Kuriyan, J. (2002) *Cell* **109,** 275–282.
22. Krupa, A., Preethi, G. & Srinivasan, N. (2004) *J. Mol. Biol.* **339,** 1025–1039.
23. Dar, A. C., Dever, T. E. & Sicheri, F. (2005) *Cell* **122,** 887–900.
24. Taylor, S. S., Haste, N. M. & Ghosh, G. (2005) *Cell* **122,** 823–825.
25. Hanks, S. K., Quinn, A. M. & Hunter, T. (1988) *Science* **241,** 42–52.
26. Dey, M., Cao, C., Dar, A. C., Tamura, T., Ozato, K., Sicheri, F. & Dever, T. E. (2005) *Cell* **122,** 901–913.
27. Dodelet, V. C. & Pasquale, E. B. (2000) *Oncogene* **19,** 5614–5619.
28. Wybenga-Groot, L. E., Baskin, B., Ong, S. H., Tong, J., Pawson, T. & Sicheri, F. (2001) *Cell* **106,** 745–757.
29. Wieser, R., Wrana, J. L. & Massague, J. (1995) *EMBO J.* **14,** 2199–2208.
30. Huse, M., Chen, Y. G., Massague, J. & Kuriyan, J. (1999) *Cell* **96,** 425–436.
31. Huse, M., Muir, T. W., Xu, L., Chen, Y. G., Kuriyan, J. & Massague, J. (2001) *Mol. Cell* **8,** 671–682.
32. Baltzis, D., Li, S. & Koromilas, A. E. (2002) *J. Biol. Chem.* **277,** 38364–38372.
33. Ibarra-Sanchez, M. J., Wagner, J., Ong, M. T., Lampron, C. & Tremblay, M. L. (2001) *Oncogene* **20,** 4728–4739.